ACS APPLIED MATERIALS & INTERFACES

Research Article

www.acsami.org

Electrospun Photochromic Hybrid Membranes for Flexible Rewritable Media

Jing Wei, Xiuling Jiao, Ting Wang,* and Dairong Chen*

School of Chemistry & Chemical Engineering; National Engineering Research Center for Colloidal Materials, Shandong University, Jinan 250100, P. R. China

Supporting Information

ABSTRACT: Ink-free rewritable media has attracted great attention as a potential alternative to current paper prints, owing to its benefits to reducing paper production and consumption for environmental protection. It is desirable to develop rewritable media based on cheap, robust, and fast-response photochromic systems. Herein, we report the design and fabrication of flexible and photorewritable PVP/a-WO_3 hybrid membranes through electrospinning, on which images with high resolution can be photoprinted and heat-erased for over 40 cycles. The well conjugated organic−inorganic hybrid structure endows a fast "electron−proton double injection" from PVP to a-WO_3 in the coloration process and greatly improves the photochromic responses. The coloration times can be as short as tens of seconds and the erasure times can be as long as 10 days in ambient conditions. As-formed photochromic membranes are low-cost, environmental benign and easy for large-scale production, indicate their great potential as flexible rewritable media for practical usage.

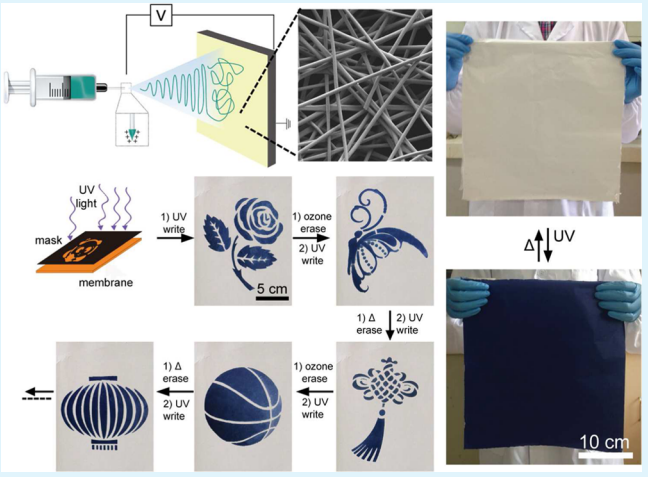

KEYWORDS: *photochromic, rewritable, electrospinning, tungsten oxide, hybrid membranes*

1. INTRODUCTION

The evolution of the information technology has greatly changed our daily lives. Large amounts of information can be shared through the Internet. However, due to the low cost of the printing setup, the amount of printed documents on paper or nonpaper substrates, such as fabrics and plastics, has still greatly increased.[1−4] The documents on paper are mostly applied in office printing while the prints on nonpaper flexible substrates are widely used as posters, banners, and signboards. Most of these prints are disposed in a short period of time, which significantly increases the business operating cost and also creates huge environmental problems. Ink-free rewritable media has attracted great attention as a potential alternative to current paper or nonpaper prints, owing to its benefits to environmental conservation and cutting down the printing cost. Previously, great efforts have been made to develop new kinds of photochromic organic dyes that undergo reversible color switching upon photoinduced isomerization.[5−9] These dyes can work as the imaging layers and be integrated with paper or nonpaper substrates as rewritable media. However, most of these organic dyes are toxic, expensive, slow in switching rates in solid state, and undergoing degradation upon continuous light stimulation. All these problems greatly hinder their practical applications. As a result, development of reliable color switching systems as rewritable media is of high priority and has gained great interest.[10−17]

Up to now, several novel photochromic systems for rewritable purpose have been developed. For example, Yin et al. successfully prepared a TiO_2-methylene blue system for rewritable purpose.[11−13] Zhang et al. prepared hydrochromic molecular switches for water-jet rewritable paper.[14] Klajn et al. proposed a novel light-controlled self-assembly of non-photoresponsive nanoparticles as rewritable media.[15] Also, some recent investigation revealed that the ultrasmall polyoxometalate (POM) clusters can work for rewritable purpose.[16,17] However, these studies are all fascinating concepts with demonstrations. The reliable large-area preparation of photochromic systems is rarely reported.

Compared with the search for new color switching systems, investigation on some conventional photochromic materials may show additional advantages upon using new methodologies or novel design. The motivation of our research is to use cheap, robust inorganic materials with low toxicity for large-scale preparation of reliable photochromic systems for rewritable purpose. Tungsten oxide (WO_3) has attractive

Received: August 23, 2016
Accepted: October 13, 2016
Published: October 13, 2016

DOI: 10.1021/acsami.6b10620
ACS Appl. Mater. Interfaces 2016, 8, 29713−29720

applications ranging from smart windows to various optoelectronics. It shows reversible color switching upon external stimuli. In an oxidizing environment, WO_3 is colorless, upon suitable stimuli, such as an electric field (electrochromic response) or UV light illumination (photochromic response), it can be switched to blue color. In this process, external electrons and metal ions (such as H^+, Li^+) are injected into the WO_3 matrix and reduce tungsten ions from 6+ to 5+. The blue color is induced by the near-infrared absorption owing to small polaron hopping.[18−21]

Up to now, investigations on electrochromic properties of WO_3 have gained tremendous progresses and some products with amorphous WO_3 films as color switching layers have been commercialized.[21−23] However, photochromic responses of traditional WO_3 films for general applications have been hampered by their slight color change, slow and irreversible photoresponse. A key to overcoming these challenges is the rational design of the WO_3 photochromic systems capable of a fast and reversible electron−ion double injection into the WO_3 substrates. Previous reports have revealed a few principles to improve the coloration efficiency: (1) amorphous or nanosize WO_3 shows much more enhanced photochromic response than bulk, crystalline WO_3, as a random defective matrix is more convenient for electron−ion intercalation, (2) compared with lithium ions, protons (H^+) can incorporate into the WO_3 substrates more easily upon light stimulation, and (3) certain organic polymers can play the role as electron donors and improve the coloration efficiency and reversibility.[24−30] Subsequently, a variety of methods have been applied in photochromic WO_3 preparation, such as chemical or physical deposition, sol−gel method.[28] Although several kinds of WO_3-based photochromic systems have been reported, their color switches were realized in solutions or gels with only slow photoresponses and slight color changes. The solid state WO_3-based color switch systems with fast photoresponses have great potential in practical usage, however, reports of them are quite rare.

Electrospinning can produce fibers with diameters ranging from mocrometers to a few nanometers and has been widely studied in the past decade. In recent years, electrospinning has been applied to prepare organic−inorganic hybrid nanofibers and various hybrid nanofibers have been prepared. Through electrospinning, the polymer with abundant active surface groups can be loaded with a very high content of inorganic components. Also, the inorganic components can be homogeneous dispersed in the polymer matrix through electrospinning.[31−33]

Herein, we report the design and fabrication of hybrid organic−inorganic fibrous membranes for flexible rewritable purpose. Amorphous WO_3 (a-WO_3) homogeneously dispersed in polyvinylpyrrolidone (PVP) has been prepared through *in situ* solution phase reaction and formed hybrid nanofibrous membranes by electrospinning. The well conjugated organic−inorganic composites promote the "electron−proton double injection" and greatly improve the photochromic responses. The coloration of the membranes can be achieved in tens of seconds using a 5 W UV lamp and the decoloration rates can be tuned by changing the membrane compositions in an oxidizing environment. Various patterns can be repeatedly printed on these membranes upon UV illumination, retained for days and spontaneously erased in ambient conditions. The printing-erasing process can be repeated for more than 40 cycles without loss in resolution. As-formed flexible membranes with excellent photochromic performance can work as rewritable media to replace regular fabric prints for environmental protection and sustainable developments.

2. RESULTS AND DISCUSSION

Fibrous membranes were produced by electrospinning of viscous hybrid solutions of ultrasmall WO_3 clusters in dimethylformamide (DMF) mixed with PVP, leading to PVP/a-WO_3 hybrid membranes (detailed experimental procedures are provided in the Experimental Section). The relative ratios of the inorganic and organic components in the membranes were tuned by changing the a-WO_3 contents from 30 wt% (W1), 50 wt% (W2), 60 wt% (W3) to 70 wt% (W4). Scanning electron microscopy (SEM) images of the hybrid membranes with various a-WO_3 contents are shown in Figure 1a−d. Electrospun nanofibers are randomly oriented and

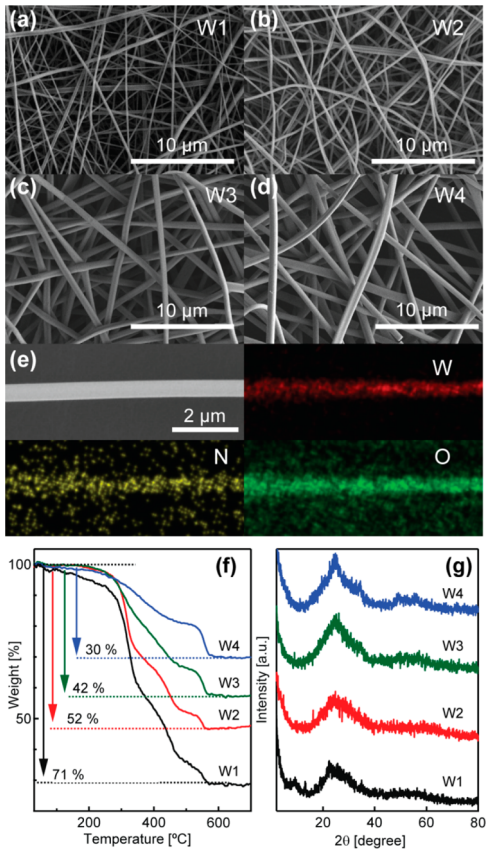

Figure 1. SEM images of the electrospun nanofibers with various a-WO_3 contents: (a) 30 wt% (W1), (b) 50 wt% (W2), (c) 60 wt% (W3), (d) 70 wt% (W4). (e) SEM image and the corresponding elemental distribution of W, N, and O. (f) TGA curves of the nanofibers with various a-WO_3 contents. (g) XRD patterns for the fibrous membranes with various a-WO_3 contents.

construct flexible membranes. The surfaces of the nanofibers are all smooth and the length of the fibers can reach to decimeter grade. Upon increasing the amount of the inorganic components, ribbon-like nanofibers instead of threadlike nanofibers are formed, and the average diameters of the nanofibers also increase from ~200 nm for W1 to ~1 μm for W4.

The elemental distribution maps of W, N, and O elements of the nanofibers (Figure 1e, Figure S1, see Supporting Information) show even distributions of the a-WO_3 and the

DOI: 10.1021/acsami.6b10620
ACS Appl. Mater. Interfaces 2016, 8, 29713−29720

organic components, which indicates the inorganic and organic parts are uniformly mixed and form one homogeneous phase. The thermal gravimetric analysis (TGA) results (Figure 1f) show marked two-step weight losses for as-prepared membranes. The initial weight losses before 450 °C associate with the decomposition of PVP components and the second stages from 450 to 550 °C relate to the dehydration and transformation of amorphous WO_3 into crystalline WO_3.[34,35] X-ray diffraction (XRD) patterns (Figure 1g) with only amorphous peaks and the electron diffraction pattern of the nanofiber (Figure S2, see Supporting Information) with no observable diffraction spots confirm the amorphous nature of the tungsten oxide in the nanofibers. We immersed 0.05 g of membranes M1-M4 individually in 50 mL distilled water and noticed the pH values of water all decreased to 5.5−6.5, indicating the membranes are all slightly acidic. Once immersed in water, membrane M1 immediately dissolved. The WO_3 in the membrane M1 may exist in the form of small clusters as the precursor solutions, once the organic PVP dissolve in water, these clusters can be dispersed and the membrane cannot maintain. However, membrane M2-M4 with higher WO_3 contents cannot dissolve in water, indicating that the initial WO_3 clusters may connect together to form an amorphous network with sharing corners or edges, owing to the increased WO_3 contents in the membranes.

The photochromic responses of the hybrid membranes were investigated upon continuous UV irradiation with a 5 W UV lamp for various irradiation times. The photographs showing the membrane color changes as a function of UV irradiation time are presented in Figure 2a. For the membrane with 30% a-WO_3, the membrane is only slightly colored after 120 s UV irradiation. With increasing WO_3 contents, the coloration processes are obviously accelerated. For the membrane with 70% WO_3, the membrane changes to a dark blue color after 120 s UV irradiation. The diffuse reflectance spectra of the hybrid membrane W4 show markedly decreased reflectance values with continuous UV irradiation and reach saturation within 2 min (Figure 2b). This coloration speed is much faster than most of the previously reported WO_3 films. The intensities of the absorbance at 700 nm in the coloration process for membranes W2−W4 with different a-WO_3 contents are presented in Figure 2c. The coloration curves are all exponential and the membranes with more a-WO_3 contents can reach higher saturation levels. For a-WO_3 contents above 70%, the electrospun nanofibers are fragile and the membranes cannot maintain. For a-WO_3 contents below 50%, the colors of the membranes are only slightly changed. Our experiments indicate that the hybrid membranes can maintain robust structures with fast and obvious color switches with 50−70% a-WO_3 contents. Also, we noticed that the thickness of the membrane can not influence the coloration process, either a thick membrane or a thin membrane showed fast color switching upon UV illumination (Figure S3, see Supporting Information).

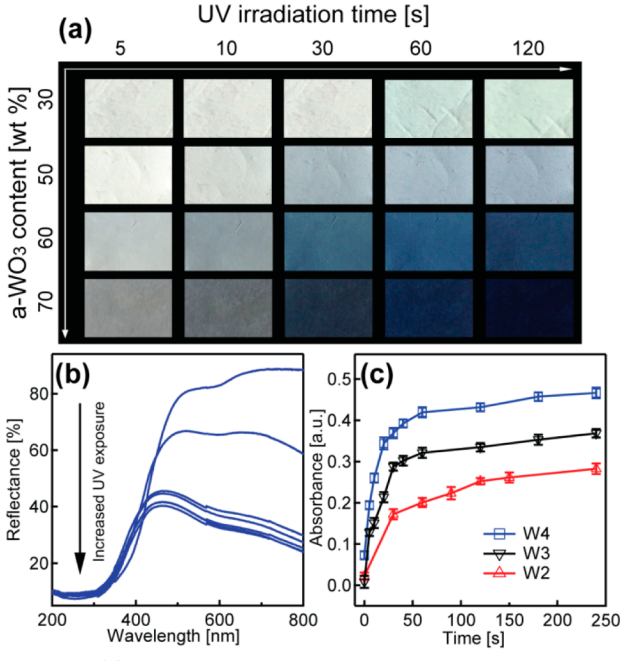

Figure 2. (a) Photographs showing the photochromic behaviors of W1−W4 as a function of the UV illumination time. (b) Reflectance spectra showing the coloration of the membrane W4 upon UV illumination under ambient conditions, recorded with 15 s interval. (c) Plots of the UV coloration process of the membranes with various a-WO_3 contents by monitoring the absorbance at 700 nm as a function of time.

IR spectra for the hybrid membranes with different a-WO_3 contents are presented in Figure S4 (see Supporting Information). In the range of 500−1000 cm^{-1}, three vibration modes are identified as W−O−W corner sharing (at 642 cm^{-1}), W−O−W edge sharing (at 810 cm^{-1}) stretching modes, and terminal oxygen stretching mode of W═O (at 975 cm^{-1}).[36] The absorption peak of the C═O group in pure PVP located at 1650 cm^{-1} shifts to higher energy in the hybrid membranes, as shown in Figure S4b (see Supporting Information). It indicates that the amorphous WO_3 might interact with the oxygen atoms of the carbonyl group in PVP to form the a-WO_3/PVP conjugates. The similar results have been obtained in other inorganic nanoparticles/PVP nanocomposites.[37,38] Since membrane W4 has showed the most obvious color changes upon UV illumination, several spectroscopic techniques have been applied to determine the structural evolution of the membrane W4 from colorless to a color state. Upon UV illumination, for membrane changes from colorless to a color state, the IR intensity for the terminal W═O stretching mode increases while the W−O−W edge-sharing and corner-sharing vibrations show decrease intensities (Figure 3a, spectra in the whole IR range are provided in Figure S5 (see Supporting Information)). One interesting observation is that we noticed a slight decrease of the water −OH vibration band upon UV illumination, which may be related with the consumption of water molecules which provides the protons for the coloration process.

Raman spectroscopy has also been employed and the spectra are shown in Figure 3b. For the colorless membrane, there are two peaks at 698 and 800 cm^{-1} representing the W−O−W stretching modes. Upon UV illumination for 30 s, these two peaks all show significant intensity decrease and with a 120 s UV illumination, these two peaks disappeared and a new band at 975 cm^{-1} appears which can be identified as the terminal W═O stretching vibration mode.[39,40] The Raman spectral changes are consistent with the IR spectral changes. Previous reports of the intercalation of lithium ions have noticed the same kind of vibration changes in the Raman spectra.[41,42] Since the coloration process relates to the proton intercalation into the tungsten oxide lattice, the intercalated protons may break

DOI: 10.1021/acsami.6b10620
ACS Appl. Mater. Interfaces 2016, 8, 29713−29720

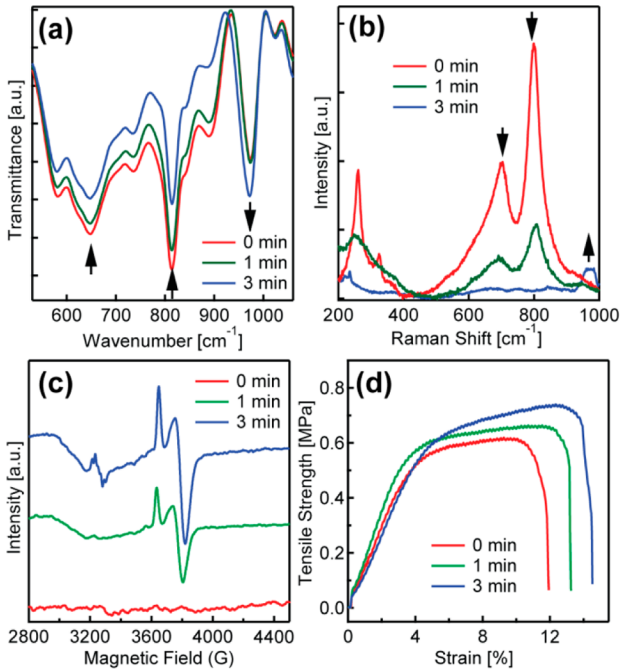

Figure 3. Comparison of the (a) IR spectra, (b) Raman spectra, (c) ESR profiles, and (d) tensile stress–strain curves for membrane W4 between before (0 min) and after (1 and 3 min) UV illumination.

the existing W–O–W bonds and form new W=O terminal bonds. The IR and Raman spectral changes in the membrane W4 prove a fast proton intercalation into the a-WO_3 network upon UV illumination.

Electron spin resonance (ESR) spectra were *in situ* measured at 108 K to verify the electronic states of W in membrane M4 in its colorless and blue color states (Figure 3c). The colorless membranes did not show any recognizable ESR signals while the blue color membrane exhibits two ESR signals, owing to the electron transfer from the organic components to the inorganic components of the membranes. The signal at about 3750 G with g = 1.71 indicates the existence of W^{5+}, the other ESR signal at 3250 G with g = 1.99 can be assigned as the organic radicals of PVP. The existence of the two ESR signals in the color membranes indicates an electron transfer process from PVP polymers to the a-WO_3 upon UV illumination.[43] Also, we believe that the C=O group in PVP is the most possible electron donor because it has been reported that PVP interacts with various nanoparticles via C=O coordination.[44−46]

In the coloration process, along with the structural evolution of the membranes, there are also significant changes in their mechanical properties. The stress–strain curves of the membranes W1–W4 and a pure PVP membrane have been presented in Figure S6 (see Supporting Information). From the stress–strain curves of membranes with different WO_3 contents we noticed that with increasing WO_3 contents the yield points are gradually diminished. Stress–strain curves were measured for several specimens of membrane W4 and the typical curves of the membrane in colorless and color states are presented in Figure 3d. The colorless membrane has a yield point with the tensile stress and tensile strain of 0.6 MPa and 10.5%. After UV illumination for 3 min, the color of the membrane turns blue and the tensile stress and the tensile strain at the yield point shift to 0.72 MPa and 13%. The improvements in tensile properties can be attributed to the structural changes of a-WO_3 in the membranes. The a-WO_3 network is composed of O–W–O bonds, upon UV illumination, the surface O–W–O bonds break into W=O ends, which increases the amount of surface active ends and promotes the interfacial interactions between PVP and a-WO_3. Also, the intercalated protons in a-WO_3 may increase the nanoscale surface roughness of the WO_3 network and enhance the mechanical interlocking with the PVP chains.

For amorphous WO_3, upon UV light illumination, the UV excited electrons reduce the W ions from 6+ to 5+ and these reduced W^{5+} ions act as color centers. These color centers absorb the incident light in the near IR region through polaron hopping between nonequivalent tungsten sites, as shown in eq 1, and for that reason the color of WO_3 switches to blue.[47−49] Recent investigations have also invoked the free electron model to explain the coloration of WO_3.[50] However, this model is only valid for the crystalline lattices. Since our hybrid membranes are highly amorphous, the polaron hopping model can be better to explain our experimental results.

$$h\nu + W_A^{5+} + W_B^{6+} \rightarrow W_B^{5+} + W_A^{6+} \quad (1)$$

Previous investigations have revealed that the coloration of a-WO_3 is an "electron–proton double injection" process (eq 2).[51,52] Upon UV illumination, protons and electrons are both intercalated into the a-WO_3 network for W reduction and structural stabilization. In our hybrid membranes, the PVP polymers work as effective electron donors while residual H^+ and structural H_2O molecules contribute the protons. A key to achieving fast photochromic response is the fast electron–proton double intercalation into tungsten oxides. Several previous reports have reported the combination of various organic surfactants or polymers with WO_3 to improve the coloration efficiency.[53−55] However, there have only been limited progress in the coloration improvement and there have been no demonstrations show a distinct and fast color switch as in this report (supplementary video in the Supporting Information), mostly owing to the low WO_3 contents in the WO_3/polymer composites, which induces slight color changes, or owing to the insufficient contact of the organic components with WO_3, which prohibits the double intercalation process.

$$xH^+ + xe^- + WO_3 \rightarrow H_xW_{1-x}^{6+}W_x^{5+}O_3 \quad (2)$$

Our hybrid membranes have two striking advantages for the electron–proton double intercalation. First, for the hybrid PVP/a-WO_3 membranes, amorphous tungsten oxides homogeneously mixed with PVP polymers and the PVP conjugated on a-WO_3 surfaces works as effective electron donors to reduce tungsten atoms upon UV illumination. Second, the hybrid membranes are slightly acidic with lots of structural H_2O molecules, therefore sufficient amounts of protons can be provided to intercalate into the a-WO_3 substrates for charge compensation, and prevent the rapid spontaneous oxidation, stabilize the blue color state. The as-prepared homogeneous hybrid membranes promote both electron transfer and proton intercalation, thus we can observe significantly improved coloration rates compared with previous reports.

A high color switching repeatability is essential for practical applications of rewritable media. As-prepared blue color membrane can become colorless upon heating in air at 80 °C for half an hour. We applied UV light illumination and heating consecutively to study the photochromic reversibility and repeatability of the hybrid membranes (Figure 4a). We noticed that the color intensity only slightly decreased after 40 coloring-

DOI: 10.1021/acsami.6b10620
ACS Appl. Mater. Interfaces 2016, 8, 29713−29720

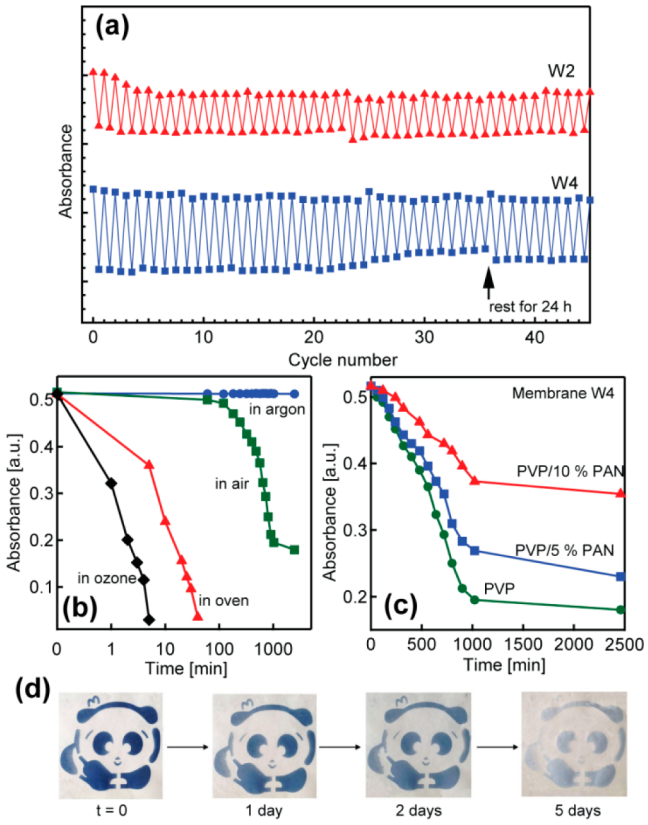

Figure 4. (a) The absorption intensity switching between color and colorless states for membranes with 50 wt% (W2) and 70 wt% (W4) a-WO_3. (b) Plots of the decoloration process for W4 in different environments by monitoring the absorption at 800 nm as a function of time: in argon gas (blue), in ambient air (green), heating at 80 °C in an oven (red), in ozone gas (black). (c) Plots of the decoloration processes for membranes with various PAN contents. (d) Erasure of a photoprinted image on the membrane (PVP/10% PAN) in ambient conditions.

erasing circles, which is significantly improved compared with the reversibility of the conventional organic rewritable systems.[14] It is worth noting that after tens of coloring-erasing cycles the tensile properties of the hybrid membrane only slightly decrease (Figure S7 see Supporting Information), and the membranes can maintain a smooth surface without noticeable cracks or defects (Figure S8 see Supporting Information). After 40 coloring-erasing cycles the membranes show a relatively slow coloration rate (a few minutes instead of 30 s toward saturation), owing to the gradual consumption and exhaustion of the PVP electron donors (IR spectra provided in Figure S9 see Supporting Information).

As shown in Figure 4b, the decoloration of the membranes can be achieved in various oxidizing environments. When sealed in a glass vial filled with argon gas, the blue color of the membrane can remain for a month without noticeable color decay. Under ambient conditions, the blue color membranes can be oxidized back to colorless in 1−2 days, while heating the membranes at 80 °C in air can transfer them to colorless in about half an hour. We noticed that it only took 5−6 min to bleach the membrane colorless when we put them in an ozone generator which can provide large amounts of oxygen radicals.[56] We also explored the effect of the a-WO_3 concentration in the membranes on the decoloration rate under ambient conditions. As shown in Figure S10 (see Supporting Information), for membranes with high a-WO_3 contents, they show significantly slower decoloration rates. For the membrane W4 with 70% a-WO_3, in ambient conditions, it takes 2 days for the membrane to be oxidized to its initial colorless state while membrane W2 only needs ∼1 day to become colorless. The decoloration rates of the membranes can be even slower by tuning the organic compositions of the hybrid membranes. Instead of PVP, we use a mixture of PVP and polyacrylonitrile (PAN) as the organic components of the membranes (Figure 4c). PAN can effectively prohibit the diffusion of O_2 to a-WO_3 inside the membranes and greatly enhance the stability of the blue color membranes in ambient conditions. By adding 10% PAN mixed with PVP to fabricate the membrane W4, the total decoloration of the membranes needs about 10 days. The tunable decoloration rates, which can retain the printed pattern for a long period of time (as shown in Figure 4d), are ideal for rewritable media which can satisfy multiple printing purposes.

The electrospun hybrid membranes can be prepared as large as 0.1−0.3 m^2 according to the size of the substrates for membrane collection (Figure 5a). The membranes are flexible

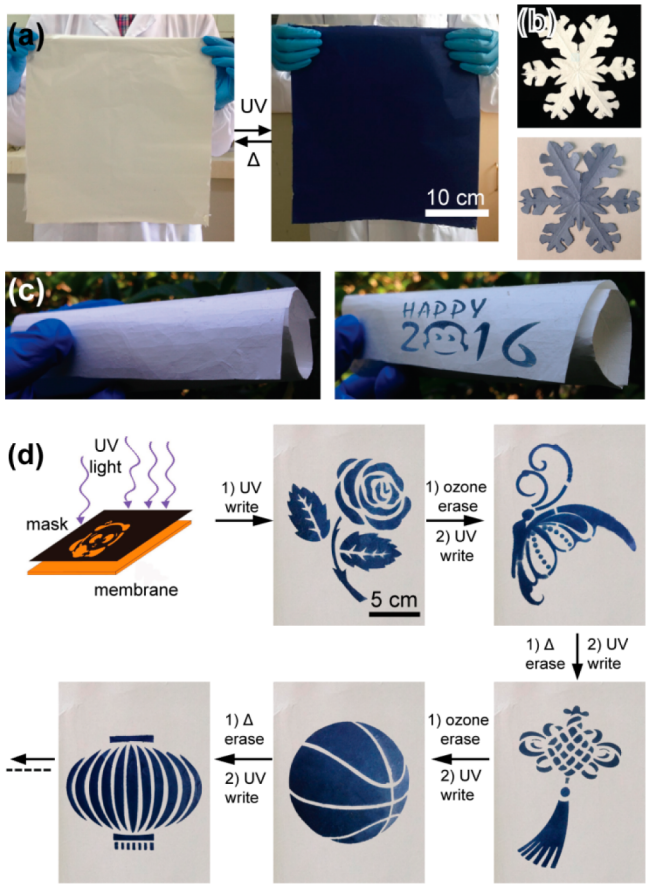

Figure 5. Rewritable and flexible membranes. (a) Photographs showing a large membrane M4 (0.3*0.3 m^2) in its colorless and color states. (b) Photographs showing a membrane M2 cut into snowflake-shape in colorless and color states, the edge of the image is 10 cm. (c) A membrane M3 can be distorted or curved without disrupting the photochromic response. (d) A series of images (cartoon figures) sequentially write into and erase from the same hybrid membrane M4. The writing times were 2 min using a 5 W UV lamp. Images were erased either by heating the membrane to 80 °C for 20 min or by exposure to ozone gas for 5 min.

DOI: 10.1021/acsami.6b10620
ACS Appl. Mater. Interfaces 2016, 8, 29713−29720

and can fold into complex structures or be cut into various shapes without losing their photochromic performances (Figure 5b, c and Figure S11 (see Supporting Information)). As a demonstration, various patterns were printed on the same membrane by UV illumination through photomasks (Figure 5d). The exposed regions on the membrane turned blue after 2 min UV illumination, and the photopatterned images gradually self-erased in a day in ambient conditions. The erasure times of the patterns can be prolonged to 10 days by changing the organic components of the membrane, and can also be accelerated by exposing to ozone or by heating in air. Once erased, the membranes can be rewritten multiple times without loss in resolution.

Currently, rewritable systems based on organic molecules, such as spiropyrans, leuco dyes, and viologens, have gained great progress and showed some unique features.[57−59] For example, for the organic chromophores, different types of organic molecules can exhibit switches between various colors upon photoisomerization while WO_3 based rewritable systems can only show color switch between colorless and blue color. However, there are also lots of advantages for our WO_3 rewritable systems over organic chromophores. One big advantage is that the erasure times for the rewritable membranes can be tuned by tuning their organic components, which have never been achieved in previous reports. Extra advantages, including the low-cost (PVP and WCl_6 are all cheap, industrially available raw materials), environmental benign, and easy for large-scale production, render them suitable for flexible rewritable media. As a demonstration, we prepared a lab coat with a "photoreprintable" pocket. The fibrous membranes stitch into the pocket of a common cotton lab coat through ultrasonic sewing technique (Figure S11 see Supporting Information). Upon UV light illumination for 2 min through a photomask, clear blue-color images can be obtained with high resolution. The photoprinted images gradually vanished after wearing the lab coat for 2 days. The images can be reprinted on the pocket and the quality of the printed images did not deteriorate within 10 print/erase cycles. Such reprintable clothes can be printed with temporary marks or advertisements for athletic purposes of sports meets and games.

3. CONCLUSION

In summary, we have described the design and fabrication of inorganic−organic hybrid membranes through electrospinning, on which images with high resolution can be photoprinted and self-erased for multiple times. Compared with the existing organic color switching systems, such as the viologens, spiropyrans, and leuco dyes, which suffer from synthetic complexity and undergo photodegradation, the electrospun hybrid membranes provide fast color switching rates, tunable color erasure times, superior reversibility, and significantly improved repeatability. Additional advantages include the easy, facile synthetic procedure, photostability, simplicity, low cost, and being environmentally benign. The applications of the hybrid photochromic membranes are far reaching, ranging from temporary prints, such as short time advertisements and posters, to large-scale photolithography and flexible rewritable optical memories. As-formed photochromic membranes have great potential as a robust rewritable system to replace regular fabric prints for sustainable developments.

4. EXPERIMENTAL SECTION

4.1. Materials. All chemicals were of analytical grade and used as received without further purification. Tungsten hexachloride (WCl_6, 99.9%) was purchased from Sigma-Aldrich. Polyvinylpyrrolidone (PVP) and polyacrylonitrile (PAN) were purchased from Bodi Chemical Co. Ltd. of Tianjin. Absolute ethanol (99.9%) and *N*,*N*-dimethylformamide (DMF) were purchased from Sinopharm Chemicals.

4.2. Fabrication of PVP/a-WO_3 Fibrous Membranes. A schematic illustration for the membrane fabrication is provided in Figure S12 (see Supporting Information). For the preparation of the a-WO_3/PVP membranes, 0.45 g PVP was dissolved in 5.0 mL DMF to form a transparent PVP solution. Various amounts of WCl_6 powder were added into the PVP solutions with vigorous stirring. These solutions were oxidized by purging oxygen gas (200 sccm) and stirred at 40 °C for 40 min to form tungsten oxide.[60] Residual H_2O in DMF reacted with WCl_6 to form HCl and evaporate out (as shown in Figure S13 in the Supporting Information), and the solution was strongly acidic with a pH value of ∼1. The color of the solution changed from colorless to jacinth and finally to a blue color owing to the formation of reduced WO_3. There was no precipitation after centrifuging the solution at 3000 rpm for 30 min, indicating there are no large WO_3 particles in the solution. The UV−vis spectra of the precursor indicates that the solution exhibited reversible color switch from colorless to blue upon UV irradiation, as shown in Figure S14 (see Supporting Information). The absorption band edge around ∼300 nm and the strong absorption peak at ∼650 nm appeared upon UV illumination all indicated that the tungsten oxide in the precursor solution is mainly in the form of small clusters,[61] which is also confirmed by the mass spectroscopy results (Figure S15 see Supporting Information). The resulting viscous hybrid solution was transformed into a 10.0 mL plastic syringe with the diameter of the needle as 0.7 mm. The flow rate of the syringe pump was 2.0 mL/h. The distance between the collector and needle was 20.0 cm. The applied voltage was held at 20 kV. The electrospun fibrous membranes were peeled off from the collector and vacuum-dried at 80 °C for 24 h to remove the DMF and other volatile residuals formed during the reaction. As-obtained membranes were pure white color and ready for further characterization.

4.3. Characterization. The field emission scanning electron microscopy (FE-SEM SU8010) images were collected to analyze the morphology and the elemental distribution of the samples. Transmission electron microscopy images (TEM) and the electron diffraction pattern were collected by JEM-1011 microscope. Powder X-ray diffraction (XRD) patterns were obtained on a Rigaku D/Max 2200pc diffractometer equipped with graphite monochromatized CuK_α radiation (λ = 0.15418 nm). The Fourier transform infrared (FT-IR) spectra were measured with a Bruker Alpha spectrometer in the range 400−4000 cm^{-1}. The Raman spectra were gathered with a micro-Raman LabRAM HR800 spectrometer. For the photochromic measurements, the coloration was measured by using a handle UV lamp (WFH-204B, Shanghai Int.) with 254 nm emission as the light source. UV−vis absorption data were collected by a Cary 100 spectrophotometer and a white standard of $BaSO_4$ was used as a reference. Electron spin resonance (ESR) spectra were obtained over Bruker ESP 300E electron paramagnetic resonance spectrometer at X-band at 108 K with in situ UV irradiation. The g-values were determined with the cwESR Simfonia Program from Bruker. Thermogravimetric measurements were measured on STA449 F3 Jupiter(NETZSCH) analyzer in air atmosphere with a heating rate of 5 °C min^{-1}. Tensile tester (XG-1A, Shanghai New Fiber Instrument Co., Ltd., China) was used to test the mechanical properties of the hybrid membranes with a champ distance of 5 mm and a drawing speed of 1 mm min^{-1}. Thermo Ultimate 3000 attached Thermo LCQ Fleet (HPLC-MS) was carried out to determine the constitutes of initial PVP/WO_3 precursor solutions.

DOI: 10.1021/acsami.6b10620
ACS Appl. Mater. Interfaces 2016, 8, 29713−29720

■ ASSOCIATED CONTENT

Supporting Information

The Supporting Information is available free of charge on the ACS Publications website at DOI: 10.1021/acsami.6b10620.

Additional SEM, TEM, and ED images; IR data and additional figures (PDF)

A video showing the coloration process of the membrane W4 (ZIP)

■ AUTHOR INFORMATION

Corresponding Authors

*E-mail: t54wang@sdu.edu.cn.

*E-mail: cdr@sdu.edu.cn.

Notes

The authors declare no competing financial interest.

■ ACKNOWLEDGMENTS

This work was supported by the Young Scholars Program of Shandong University (YSPSDU, No. 2015WLJH27) and the Fundamental Research Funds (No. 2015TB004) of Shandong University, also funded by the Taishan Scholars Climbing Program of Shandong Province (tspd20150201).

■ REFERENCES

(1) Allen-Robertson, J. The Materiality of Digital Media: The Hard Disk Drive, Phonograph, Magnetic Tape and Optical Media in Technical Close-up. *New Media Soc.* **2015**, DOI: 10.1177/1461444815606368.

(2) Hotta, Y. Rewritable Marking Technology. *Nihon Gazo Gakkaishi/Journal of the Imaging Society of Japan* **2012**, *51*, 213–222.

(3) Fletcher, K. *Sustainable Fashion and Textiles: Design Journeys*; Routledge, 2013.

(4) Ashby, M. F. *Materials and the Environment: Eco-informed Material Choice*; Elsevier, 2012.

(5) Kanazawa, K.; Nakamura, K.; Kobayashi, N. Electroswitchable Optical Device Enabling both Luminescence and Coloration Control Consisted of Fluoran Dye and 1, 4-Benzoquinone. *Sol. Energy Mater. Sol. Cells* **2016**, *145*, 42–53.

(6) Nagy, V.; Suleimanov, I.; Molnár, G.; Salmon, L.; Bousseksou, A.; Csóka, L. Cellulose-Spin Crossover Particle Composite Papers with Reverse Printing Performance: a Proof of Concept. *J. Mater. Chem. C* **2015**, *3*, 7897–7905.

(7) Garcia-Amorós, J.; Swaminathan, S.; Raymo, F. M. Saving Paper With Switchable Ink. *Dyes Pigm.* **2014**, *106*, 71–73.

(8) Kawashima, I.; Takahashi, H.; Hirano, S.; Matsushima, R. A Photon-Mode Full-Color Rewritable Image Using Photochromic Compounds. *J. Soc. Inf. Disp.* **2004**, *12*, 81–85.

(9) Zhang, J. J.; Zou, Q.; Tian, H. Photochromic Materials: More than Meets the Eye. *Adv. Mater.* **2013**, *25*, 378–399.

(10) Zeng, L. C.; Pan, F. S.; Li, W. H.; Jiang, Y.; Zhong, X. W.; Yu, Y. Free-Standing Porous Carbon Nanofibers-Sulfur Composite for Flexible Li-S Battery Cathode. *Nanoscale* **2014**, *6*, 9579–9587.

(11) Wang, W. S.; Xie, N.; He, L.; Yin, Y. D. Photocatalytic Colour Switching of Redox Dyes for Ink-Free Light-Printable Rewritable Paper. *Nat. Commun.* **2014**, *5*, 5459.

(12) Wang, W. S.; Ye, Y.; Feng, J.; Chi, M. F.; Guo, J. H.; Yin, Y. D. Enhanced Photoreversible Color Switching of Redox Dyes Catalyzed by Barium-Doped TiO_2 Nanocrystals. *Angew. Chem.* **2015**, *127*, 1337–1342.

(13) Wang, W. S.; Ye, M. M.; He, L.; Yin, Y. D. Nanocrystalline TiO_2-Catalyzed Photoreversible Color Switching. *Nano Lett.* **2014**, *14*, 1681–1686.

(14) Sheng, L.; Li, M.; Zhu, S. Y.; Li, H.; Xi, G.; Li, Y. G.; Wang, Y.; Li, Q. S.; Liang, S. J.; Zhong, K.; Zhang, S. X. A. Hydrochromic Molecular Switches for Water-jet Rewritable Paper. *Nat. Commun.* **2014**, *5*, 3044.

(15) Kundu, P. K.; Samanta, D.; Leizrowice, R.; Margulis, B.; Zhao, H.; Börner, M.; Klajn, R.; Udayabhaskararao, D.; Manna, R. Light-Controlled Self-assembly of Non-Photoresponsive Nanoparticles. *Nat. Chem.* **2015**, *7*, 646–652.

(16) Sun, H. J.; Gao, N.; Ren, J. S.; Qu, X. G. Polyoxometalate-Based Rewritable Paper. *Chem. Mater.* **2015**, *27*, 7573–7576.

(17) Wang, C.; Zhou, B. P.; Zeng, X. P.; Hong, Y. Y.; Gao, Y. B.; Wen, W. J. Enhanced Photochromic Efficiency of Transparent and Flexible Nanocomposite Films Based on PEO–PPO–PEO and Tungstate Hybridization. *J. Mater. Chem. C* **2015**, *3*, 177–186.

(18) Hersh, H. N.; Kramer, W. E.; McGee, J. H. Mechanism of Electrochromism in WO_3. *Appl. Phys. Lett.* **1975**, *27*, 646–648.

(19) Granqvist, C. G. Oxide Electrochromics: An Introduction to Devices and Materials. *Sol. Energy Mater. Sol. Cells* **2012**, *99*, 1–13.

(20) Deb, S. K. Opportunities and Challenges in Science and Technology of WO_3 for Electrochromic and Related Applications. *Sol. Energy Mater. Sol. Cells* **2008**, *92*, 245–258.

(21) Granqvist, C. G. Electrochromics for Smart Windows: Oxide-Based Thin Films and Devices. *Thin Solid Films* **2014**, *564*, 1–38.

(22) Jensen, J.; Hösel, M.; Dyer, A. L.; Krebs, F. C. Development and Manufacture of Polymer-Based Electrochromic Devices. *Adv. Funct. Mater.* **2015**, *25*, 2073–2090.

(23) Cong, S.; Tian, Y. Y.; Li, Q. W.; Zhao, Z. G.; Geng, F. X. Single-Crystalline Tungsten Oxide Quantum Dots for Fast Pseudocapacitor and Electrochromic Applications. *Adv. Mater.* **2014**, *26*, 4260–4267.

(24) Schirmer, O. F.; Wittwer, V.; Baur, G.; Brandt, G. Dependence of WO_3 Electrochromic Absorption on Crystallinity. *J. Electrochem. Soc.* **1977**, *124*, 749–753.

(25) Bechinger, C.; Oefinger, G.; Herminghaus, S.; Leiderer, P. On the Fundamental Role of Oxygen for the Photochromic Effect of WO_3. *J. Appl. Phys.* **1993**, *74*, 4527–4533.

(26) Shigesato, Y. Photochromic Properties of Amorphous WO_3 Films. *Jpn. J. Appl. Phys.* **1991**, *30*, 1457.

(27) Ozkan, E.; Lee, S. H.; Tracy, C. E.; Pitts, J. R.; Deb, S. K. Comparison of Electrochromic Amorphous and Crystalline Tungsten Oxide Films. *Sol. Energy Mater. Sol. Cells* **2003**, *79*, 439–448.

(28) He, T.; Yao, J. N. Photochromic Materials Based on Tungsten Oxide. *J. Mater. Chem.* **2007**, *17*, 4547–4557.

(29) Zhang, G. G.; Yang, W. S.; Yao, J. N. Thermally Enhanced Visible-Light Photochromism of Phosphomolybdic Acid-Polyvinylpyrrolidone Hybrid Films. *Adv. Funct. Mater.* **2005**, *15*, 1255–1259.

(30) Yano, S.; Kurita, K.; Iwata, K.; Furukawa, T.; Kodomari, M. Structure and Properties of Poly (vinyl alcohol)/Tungsten Trioxide Hybrids. *Polymer* **2003**, *44*, 3515–3522.

(31) Shao, C. L.; Kim, H. Y.; Gong, J.; Ding, B.; Lee, D. R.; Park, S. J. Fiber Mats of Poly (vinyl alcohol)/Silica Composite via Electrospinning. *Mater. Lett.* **2003**, *57*, 1579–1584.

(32) Pinto, N. J.; González, R.; Johnson, A. T.; MacDiarmid, A. G. Electrospun Hybrid Organic/Inorganic Semiconductor Schottky Aanodiode. *Appl. Phys. Lett.* **2006**, *89*, 033505.

(33) Sui, X. M.; Shao, C. L.; Liu, Y. C. White-Light Emission of Polyvinyl alcohol/ ZnO Hybrid Nanofibers Prepared by Electrospinning. *Appl. Phys. Lett.* **2005**, *87*, 113115.

(34) Zheng, M. P.; Gu, M. Y.; Jin, Y. P.; Jin, G. L. Preparation, Structure and Properties of TiO_2–PVP Hybrid Films. *Mater. Sci. Eng., B* **2000**, *77*, 55–59.

(35) Chen, X. C.; Lin, Y. X. Photochromism of Peroxotungstic Acid/PVP Nanocomposite Obtained by Sol-Gel Method. *J. Sol-Gel Sci. Technol.* **2005**, *36*, 197–201.

(36) Gao, G. H.; Zhang, Z. H.; Wu, G. M.; Jin, X. B. Engineering of Coloration Responses of Porous WO_3 Gasochromic Films by Ultraviolet Irradiation. *RSC Adv.* **2014**, *4*, 30300–30307.

(37) Zou, P.; Hong, X.; Ding, Y.; Zhang, Z. Y.; Chu, X. Y.; Shaymurat, T.; Shao, C. L.; Liu, Y. C. Up-Conversion Luminescence of $NaYF_4$: Yb^{3+}/Er^{3+} Nanoparticles Embedded into PVP Nanotubes with Controllable Diameters. *J. Phys. Chem. C* **2012**, *116*, 5787–5791.

(38) Lu, X. F.; Zhao, Y. Y.; Wang, C. Fabrication of PbS Nanoparticles in Polymer-Fiber Matrices by Electrospinning. *Adv. Mater.* **2005**, *17*, 2485−2488.
(39) Santato, C.; Odziemkowski, M.; Ulmann, M.; Augustynski, J. Crystallographically Oriented Mesoporous WO_3 Films: Synthesis, Characterization, and Applications. *J. Am. Chem. Soc.* **2001**, *123*, 10639−10649.
(40) He, Y. P.; Zhao, Y. P. Near-Infrared Laser-Induced Photothermal Coloration in $WO_3{\cdot}H_2O$ Nanoflakes. *J. Phys. Chem. C* **2008**, *112*, 61−68.
(41) Balaji, S.; Djaoued, Y.; Albert, A. S.; Ferguson, R. Z.; Brüning, R. Hexagonal Tungsten Oxide Based Electrochromic Devices: Spectroscopic Evidence for the Li Ion Occupancy of Four-Coordinated Square Windows. *Chem. Mater.* **2009**, *21*, 1381−1389.
(42) Balaji, S.; Djaoued, Y.; Albert, A. S.; Brüning, R.; Beaudoin, N.; Robichaud, J. Porous Orthorhombic Tungsten Oxide Thin Films: Synthesis, Characterization, and Application in Electrochromic and Photochromic Devices. *J. Mater. Chem.* **2011**, *21*, 3940−3948.
(43) Kleperis, J. J.; Cikmach, P. D.; Lusis, A. R. Colour Centres in Amorphous Tungsten Trioxide Thin Films. *Phys. Status Solidi A* **1984**, *83*, 291−297.
(44) Qiu, L. M.; Liu, F.; Zhao, L. Z.; Yang, W. S.; Yao, J. N. Evidence of a Unique Electron Donor-Acceptor Property for Platinum Nanoparticles as Studied by XPS. *Langmuir* **2006**, *22*, 4480−4482.
(45) Tsunoyama, H.; Ichikuni, N.; Sakurai, H.; Tsukuda, T. Effect of Electronic Structures of Au Clusters Stabilized by Poly (N-vinyl-2-pyrrolidone) on Aerobic Oxidation Catalysis. *J. Am. Chem. Soc.* **2009**, *131*, 7086−7093.
(46) Tseng, R. J.; Baker, C. O.; Shedd, B.; Huang, J.; Kaner, R. B.; Ouyang, J.; Yang, Y. Charge Transfer Effect in the Polyaniline-Gold Nanoparticle Memory System. *Appl. Phys. Lett.* **2007**, *90*, 053101.
(47) Berggren, L.; Azens, A.; Niklasson, G. A. Polaron Absorption in Amorphous Tungsten Oxide Films. *J. Appl. Phys.* **2001**, *90*, 1860−1863.
(48) Granqvist, C. G. Electrochromic Oxides: A Aandstructure Approach. *Sol. Energy Mater. Sol. Cells* **1994**, *32*, 369−382.
(49) Antonaia, A.; Polichetti, T.; Addonizio, M. L.; Aprea, S.; Minarini, C.; Rubino, A. Structural and Optical Characterization of Amorphous and Crystalline Evaporated WO_3 Layers. *Thin Solid Films* **1999**, *354*, 73−81.
(50) Manthiram, K.; Alivisatos, A. P. Tunable Localized Surface Plasmon Resonances in Tungsten Oxide Nanocrystals. *J. Am. Chem. Soc.* **2012**, *134*, 3995−3998.
(51) Faughnan, B. W.; Crandall, R. S.; Lampert, M. A. Model for the Bleaching of WO_3 Electrochromic Films by An Electric Field. *Appl. Phys. Lett.* **1975**, *27*, 275−277.
(52) Crandall, R. S.; Faughnan, B. W. Dynamics of Coloration of Amorphous Electrochromic Films of WO_3 at Low Voltages. *Appl. Phys. Lett.* **1976**, *28*, 95−97.
(53) Chen, Z. H.; Yang, Y. A.; Qiu, J. B.; Yao, J. N. Fabrication of Photochromic WO_3/4,4′-BAMBp Superlattice Films. *Langmuir* **2000**, *16*, 722−725.
(54) Zhang, G. J.; Chen, Z. H.; He, T.; Ke, H. H.; Ma, Y.; Shao, K.; Yang, W. S.; Yao, J. N. Construction of Self-assembled Ultrathin Polyoxometalate/1, 10-Decanediamine Photochromic Films. *J. Phys. Chem. B* **2004**, *108*, 6944−6948.
(55) Yamazaki, S.; Ishida, H.; Shimizu, D.; Adachi, K. Photochromic Properties of Tungsten Oxide/Methylcellulose Composite Film Containing Dispersing Agents. *ACS Appl. Mater. Interfaces* **2015**, *7*, 26326−26332.
(56) Wei, J.; Jiao, X. L.; Wang, T.; Chen, D. R. The Fast and Reversible Intrinsic Photochromic Response of Hydrated Tungsten Oxide Nanosheets. *J. Mater. Chem. C* **2015**, *3*, 7597−7603.
(57) Berkovic, G.; Krongauz, V.; Weiss, V. Spiropyrans and Spirooxazines for Memories and Switches. *Chem. Rev.* **2000**, *100*, 1741−1754.
(58) *Chemistry and Applications of Leuco Dyes*; Springer Science & Business Media, 2006.
(59) Beaujuge, P. M.; Reynolds, J. R. Color Control in π-Conjugated Organic Polymers for Use in Electrochromic Devices. *Chem. Rev.* **2010**, *110*, 268−320.
(60) Zhang, J.; Wessel, S. A.; Colbow, K. Spray Pyrolysis Elecrochromic WO_3 Films: Electrical and X-ray Diffraction Measurements. *Thin Solid Films* **1990**, *185*, 265−277.
(61) Renneke, R. F.; Kadkhodayan, M.; Pasquali, M.; Hill, C. L. Roles of Surface Protonation on the Photodynamic, Catalytic, and Other Properties of Polyoxometalates Probed by the Photochemical Functionalization of Alkanes. Implications for Irradiated Semiconductor Metal Oxides. *J. Am. Chem. Soc.* **1991**, *113*, 8357−8367.

DOI: 10.1021/acsami.6b10620
ACS Appl. Mater. Interfaces 2016, 8, 29713−29720